Quantum dynamics of semiconductor quantum dot Josephson junctions

Utkan Güngördü,[1,2,*] Rusko Ruskov,[1,2] Silas Hoffman,[1] Kyle Serniak,[3,4] Andrew J. Kerman,[3] and Charles Tahan[1,†]

[1]*Laboratory for Physical Sciences, 8050 Greenmead Drive, College Park, Maryland 20895, USA*
[2]*Department of Physics, University of Maryland, College Park, Maryland 20742, USA*
[3]*Lincoln Laboratory, Massachusetts Institute of Technology, Lexington, Massachusetts 02421, USA*
[4]*Research Laboratory of Electronics, Massachusetts Institute of Technology, Cambridge, Massachusetts 02139, USA*

(Received 29 March 2024; revised 5 September 2024; accepted 20 May 2025; published 2 June 2025)

Josephson junctions constructed from superconductor-semiconductor-superconductor heterostructures have been used to realize a variety of voltage-tunable superconducting quantum devices, including qubits and parametric amplifiers. To date, theoretical descriptions of these systems have been restricted to small quantum fluctuations of the junction phase, making them inapplicable to many experiments. In this paper, we relax this, employing a path-integral formulation where the phase quantum dynamics is obtained self-consistently from an underlying many-body formalism. Our method recovers previously known results for small phase fluctuations, and predicts effects outside of that limit: (i) system capacitances undergo a gate-voltage-dependent renormalization; and (ii) an additional charge offset appears for asymmetric junctions. Our main results can be summarized in terms of a single-particle Hamiltonian, which can be directly compared to that of an ordinary Josephson junction. This more general theory could be a first step towards designing new quantum devices that go qualitatively beyond voltage-tunable variants of previously known circuits.

DOI: 10.1103/PhysRevB.111.214503

I. INTRODUCTION

Superconducting circuits based on Josephson junctions (JJs) have been used to realize a variety of devices, including quantum amplifiers, digital logic circuits, and photon detectors. The most intensively studied applications of these circuits, however, are qubits, making them one of the promising and fastest-growing platforms for realizing large-scale quantum information processors [1,2]. Many different JJ-based qubits have been demonstrated, including the transmon [3], flux qubit [4], fluxonium [5], and $0-\pi$ qubit [6]. The JJs of these circuits have most often been based on superconductor-insulator-superconductor (S-I-S) tunnel junctions; however, high-quality superconductor-semiconductor (super-semi) heterostructure JJs have also recently been realized in a variety of materials. These super-semi junctions, while exhibiting the Josephson effect, carry critical currents that are tunable via the field effect of an electrostatic gate, allowing a new class of voltage-tunable quantum circuits such as the gatemon [7–9], Andreev-pair qubits [10,11], and Andreev spin qubits [12,13]. These devices have also served as a testbed for the underlying Andreev physics of superconducting weak links, and more recently, as building blocks of new topologically nontrivial superconducting circuits [14,15].

Much of the theory of super-semi junctions has built upon the Bogoliubov–de Gennes picture of Andreev transport in superconducting-normal-superconducting junctions [16], with extensions for the practically relevant situation in which an electrostatic disorder potential forms a quantum dot in the junction. The low-energy dynamics of these S-QD-S junctions have been studied in circuits where the junction is shunted by a small inductance, wherein the gauge-invariant phase difference between superconducting electrodes is set, apart from small quantum fluctuations, by the external flux through the inductance [17,18]. This regime is relevant for Andreev qubits. However, these theories do not extend to S-QD-S junctions embedded in arbitrary circuit environments that may support strong quantum phase fluctuations across the junction (e.g., transmon or fluxonium circuits).

In this paper, we develop a microscopic theory of a S-QD-S junction embedded in a capacitive environment in which quantum fluctuations of the phase may be large. Our self-consistent treatment of quantum dynamics of the superconducting phases reveal two effects that originate from the underlying many-body physics: (i) a renormalization of the effective capacitance that shunts the junction, and (ii) appearance of an additional charge offset in the charging energy for asymmetric junctions. The dependence of both effects on junction gate voltage makes them important for the analysis, control, and design of superconducting circuits with S-QD-S junctions.

II. MANY-BODY TREATMENT OF SUPERCONDUCTING CIRCUITS

In the phenomenology of JJs and circuit quantization [19,20], JJs are treated as nonlinear inductors, and quantization is postulated from the corresponding classical Hamiltonian of the circuit [20]. Within this framework, the

*Contact author: utkan@lps.umd.edu
†Present address: Department of Physics, University of Maryland, College Park, Maryland 20742, USA.

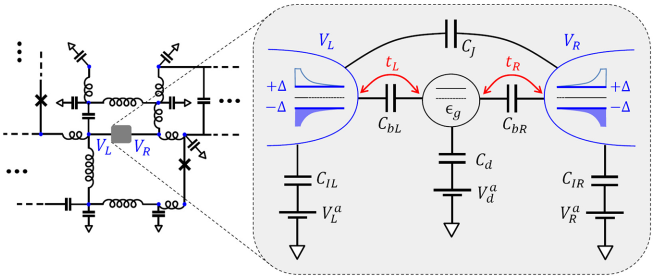

FIG. 1. A capacitively shunted S-QD-S junction embedded in a general circuit environment that does not restrict phase dynamics. The leads (blue, with BCS density of states) are tunnel coupled via t_L, t_R to the QD (containing a single level). C_J is the capacitance between the leads, and C_{bL}, C_{bL} are capacitances between the dot and each lead. V_L and V_R denote the mean-field voltage variables for each lead, and ϵ_g is the effective energy of the dot level, derived in the text. V_L^a, V_R^a, V_d^a are externally applied voltages across capacitances C_{IL}, C_{IR}, C_d, respectively. For simplicity, we consider a symmetric capacitance arrangement, $C_{bL} = C_{bR} = C_b$, $C_{IL} = C_{IR} = C_I$.

well-known Hamiltonian for a capacitively shunted JJ (such as a Cooper pair box (CPB) or transmon [3]) is obtained as

$$\hat{H}_{\text{CPB}} = \frac{(2e)^2}{2C_\Sigma}[\hat{n} - n_g(V^a)]^2 - E_J\cos(\hat{\phi}), \tag{1}$$

reflecting the quantum mechanics of the phase difference between the two superconducting leads $\phi \equiv \phi_L - \phi_R$, where the phase ϕ plays the role of a "coordinate" for the Josephson potential, and the charging energy looks like a classical expression with shunting capacitance C_Σ, a dimensionless charge operator, $\hat{n} \equiv -i\partial_\phi$, and a charge offset $n_g(V^a)$ associated with an externally applied voltage V^a.

This Hamiltonian $\hat{H}_{\text{CPB}}$ can be derived self-consistently from an underlying many-body theory in which a pair of tunnel-coupled superconducting leads are described by BCS Hamiltonians, and charging energy is introduced in a many-body picture. This program was realized in a seminal paper by Ambegaokar, Eckern, and Schön [21], where the path-integral formulation of a (grand canonical) partition function $Z_G \propto \text{tr}e^{-\beta\hat{H}}$ ($\beta = 1/k_BT$ is the inverse temperature) is evaluated at a saddle point, generating (self-consistently) the superconducting order parameters of the leads $\Delta e^{i\phi_{L,R}}$, and the voltage drop across the junction $V = V_L - V_R$, both in a mean-field approach. The partition function is then reduced to an effective action $Z_G \sim \int \mathcal{D}\phi e^{-\frac{S[\phi(\tau)]}{\hbar}}$, from which the Hamiltonian $\hat{H}_{\text{CPB}}$ can be deduced under the "slow phase approximation" in which $\phi(\tau)$ varies slowly over the time scale $\tau \sim \hbar/\Delta$. In the next order of slow phase expansion, Eckern *et al.* [22], and Larkin and Ovchinnikov [23], derived a small renormalization of the shunting capacitance across the junction $\delta C_\Sigma^{\text{JJ}} = 3\pi\hbar/(32\Delta R_N)$, where R_N is the normal state resistance of the junction [22]. This capacitance does not significantly alter the quantization prescription for such circuits [20]; at the same time its smallness makes it difficult to measure experimentally.

To summarize the results of this paper, we use the formalism of Refs. [21,22] to describe a S-QD-S junction in a capacitive environment (inset of Fig. 1) and obtain an effective Hamiltonian with a form that is similar to $\hat{H}_{\text{CPB}}$, given by

$$\hat{H}_{\text{even}} = \frac{(2e)^2}{2(C_\Sigma + \delta C_\Sigma)}[\hat{n} - \hat{n}_q(V^a, \Gamma_{L,R}, \epsilon_g, \Delta)]^2 + \hat{U}_J(\phi, \Gamma_{L,R}, \epsilon_g, \Delta). \tag{2}$$

Here, the Josephson potential $\hat{U}_J$, and the charging Hamiltonian are matrices acting on the even occupancy (singlet) space of the dot $\{|0\rangle, |\uparrow\downarrow\rangle\}$, and depend on the dot's gate voltage ϵ_g, and the tunneling rates $\Gamma_{L,R}$ between the leads and the dot. The *derived* charge offset ($\hat{n}_q$) differs from the *assumed* form (n_g) in the literature [24–26]: it contains new terms that depend on tunneling asymmetry and dot occupation (proportional to the Pauli matrices η_0 and η_z), moreover, the capacitance renormalization $\delta C_\Sigma(\Gamma_{L,R}, \epsilon_g, \Delta)$ is gate-voltage tunable. The Josephson potential matrix $\hat{U}_J$, whose eigenvalues determine the Andreev bound states (ABS) spectrum, essentially coincides with the results of [18], with the addition of nonperturbative corrections for finite dot voltage ϵ_g.

III. MODEL

By quantizing the classical Hamiltonian of the circuit shown in the inset of Fig. 1 and combining it with the junction Hamiltonian, we obtain $\hat{H} = \hat{H}_J + \hat{H}_Q$, where

$$\begin{aligned}\hat{H}_J &= \sum_{i=L,R,\sigma=\uparrow,\downarrow}\int dr\Big(\hat{\psi}^\dagger_{i,\sigma}\hat{\xi}_i\hat{\psi}_{i,\sigma} - \frac{g}{2}\hat{\psi}^\dagger_{i,\sigma}\hat{\psi}^\dagger_{i,-\sigma}\hat{\psi}_{i,-\sigma}\hat{\psi}_{i,\sigma}\Big)\\ &\quad + \hat{d}^\dagger_\sigma\mu_d\hat{d}_\sigma + (t_i\hat{d}^\dagger_\sigma\hat{\psi}_{i,\sigma}(r=0) + \text{H.c}),\\ \hat{H}_Q &= \frac{1}{2C_\Sigma}\left(\frac{\hat{Q}_L - \hat{Q}_R}{2}\right)^2 - \frac{1}{C_\Sigma}\left(\frac{\hat{Q}_L - \hat{Q}_R}{2}\right)\Delta Q + \epsilon_d\frac{1}{e}\hat{Q}_d\\ &\quad + \frac{1}{e^2}U\hat{Q}_d^2.\end{aligned} \tag{3}$$

$\hat{H}_J$ models the junction (dot and leads) and $\hat{H}_Q$ describes a capacitive circuit environment in terms of the charges $\hat{Q}_i = \sum_\sigma e\int dr\hat{\psi}^\dagger_{i,\sigma}\hat{\psi}_{i,\sigma}$ and $\hat{Q}_d = \sum_\sigma e\hat{d}^\dagger_\sigma\hat{d}_\sigma$. The fermionic field operators for the leads and dot are respectively $\hat{\psi}_{i,\sigma} = \hat{\psi}_{i,\sigma}(r)$ and $\hat{d}_\sigma$ with spin σ, where the dot is modeled as having a single accessible level [27]. Above, $\hat{\xi}_i = \frac{\hat{p}^2}{2m^*} - \mu_i$ is the kinetic-energy operator for the leads with effective mass m^*, μ_i, and μ_d are chemical potentials for isolated leads and dot, g is the strength of the BCS pair potential around the Fermi level, and t_i is the tunneling strength between the leads and the dot. The capacitance across the junction $C_\Sigma = C_J + \frac{C_b+C_I}{2}$, the charging energy of the dot $U = \frac{e^2}{4(C_b+\frac{C_dC_I}{C_d+2C_I})}$, the charge offset, $\Delta Q = \frac{C_I}{2}V^a$ owing to an applied voltage $V^a = V_R^a - V_L^a$, and the shift in the dot level $\epsilon_d = \frac{4U}{e}\frac{C_IC_d}{2C_I+C_d}(V_d^a - \frac{V_R^a+V_L^a}{2})$, are because of the electrostatic environment.

To capture the quantum dynamics of the phase difference between the electrodes, we express the partition function of the system, $Z_G = \text{tr}e^{-\beta\hat{H}}$, as an imaginary-time ($\tau$) fermionic coherent state path integral [17,21,23,28,29]. We eliminate all quartic interaction terms using the Hubbard–Stratonovich transformation at the expense of introducing auxiliary bosonic fields $\Delta(\tau)e^{i\phi_i(\tau)}$, $V_i(\tau)$, and $M(\tau)$, representing the s-wave superconducting order parameters [21,22,28], the voltage of the leads, and the magnetic Weiss field [29,30], respectively, followed by saddle point approximations that pin $\Delta(\tau) \to \Delta$, $i\hbar\partial_\tau\phi_i(\tau) \to 2eV_i(\tau)$ (i.e., Josephson relation), and $M(\tau) \to M$. From self-consistent calculations [30], we find the saddle-point value of M approximately vanishes for even occupancy states of the dot at any phase and outside the Kondo regime, i.e., for $\Delta \gg T_K = \sqrt{\frac{U\Gamma}{2}}e^{-\frac{\pi}{8U\Gamma}|U^2-4\epsilon_g^2|}$ where $\Gamma \equiv \Gamma_L + \Gamma_R$ [31]. Henceforth, unless otherwise noted, we restrict our analysis to the even occupancy sector and to a set of parameters that are outside the Kondo regime. Consequently, we take $M = 0$, so the overall effect of the Coulomb interaction is a shift of the dot level [32] by $\frac{U}{2}$, which is contained in the definition of $\epsilon_g = \epsilon_d + \mu_d + \frac{U}{2}$.

Performing a unitary transformation that shifts all time dependence owing to $\phi_i(\tau)$ onto the tunneling terms from the leads [22], we obtain

$$Z_G = \int \mathcal{D}\phi_L\mathcal{D}\phi_R\mathcal{D}^2\Psi e^{-\frac{1}{\hbar}\int_0^{\hbar\beta}d\tau\sum_{\boldsymbol{k}}\bar{\Psi}(\boldsymbol{k},\tau)[-G^{-1}(\boldsymbol{k},\tau)]\Psi(\boldsymbol{k},\tau)}$$
$$\times e^{\frac{1}{\hbar}\int_0^{\hbar\beta}d\tau\frac{C_\Sigma}{2}\left(V(\tau)+\frac{C_I}{2C_\Sigma}V^a\right)^2}e^{-\beta\frac{M^2}{2U}}, \text{ with}$$
$$-G^{-1}(\boldsymbol{k},\tau) = \hbar\partial_\tau +$$
$$\begin{pmatrix} \xi_{L,\boldsymbol{k}}\tau_z + \Delta\tau_x & 0 & \frac{t_L}{\sqrt{\mathcal{V}_L}}\tau_z e^{-i\tau_z\frac{\phi_L(\tau)}{2}} \\ 0 & \xi_{R,\boldsymbol{k}}\tau_z + \Delta\tau_x & \frac{t_R}{\sqrt{\mathcal{V}_R}}\tau_z e^{-i\tau_z\frac{\phi_R(\tau)}{2}} \\ \frac{t_L}{\sqrt{\mathcal{V}_L}}\tau_z e^{i\tau_z\frac{\phi_L(\tau)}{2}} & \frac{t_R}{\sqrt{\mathcal{V}_R}}\tau_z e^{i\tau_z\frac{\phi_R(\tau)}{2}} & \epsilon_g\tau_z + M \end{pmatrix} \quad (4)$$

where $G(\boldsymbol{k},\tau)$ is the Green's function of the junction in a momentum representation, the term $\propto C_\Sigma$ is the capacitive energy with $V(\tau) = V_L(\tau) - V_R(\tau) = \frac{\hbar}{2e}i\partial_\tau\phi(\tau)$, and $\Psi(\boldsymbol{k},\tau) = \Psi = (\psi_L, \psi_R, D)^T$, where $\psi_i = (\psi_{i,\uparrow}, \bar{\psi}_{i,\downarrow})^T$, $D = (d_\uparrow, \bar{d}_\downarrow)^T$ are Grassmann–Nambu spinors, and $\mathcal{V}_i$ is the volume of each lead. We proceed to obtain a description of the ABS, which have contributions from in-gap and continuum energies.

IV. IN-GAP CONTRIBUTIONS

By integrating out the fermionic fields $\psi_i(\boldsymbol{k},\tau)$ of the leads while retaining the $D(\tau)$ field, we derive an effective action of the dot,

$$S_E = \int_0^{\hbar\beta}d\tau\left[\int_0^{\hbar\beta}d\tau'\bar{D}(\tau)\left[-G_{dd}^{-1}(\tau,\tau')\right]D(\tau')\right.$$
$$\left.-\frac{C_\Sigma}{2}\left(\frac{\hbar}{2e}i\partial_\tau\phi(\tau) + \frac{C_I}{2C_\Sigma}V^a\right)^2\right]. \quad (5)$$

In the Green's function $-G_{dd}^{-1}(\tau,\tau') = (\hbar\partial_\tau + \epsilon_g\tau_z)\delta(\tau - \tau') + \Sigma(\tau,\tau')$, the first term captures the isolated dot, and the self-energy term $\Sigma(\tau,\tau') = \sum_i t_i^2 e^{i\tau_z\frac{\phi_i(\tau)}{2}}\tau_z g_i(\tau - \tau')\tau_z e^{-i\tau_z\frac{\phi_i(\tau')}{2}}$ captures the coupling to the leads, where $g_i(\tau) \approx \sum_n(-\pi\nu_i\frac{\hbar\omega+\Delta\tau_x}{\sqrt{\Delta^2-(\hbar\omega)^2}})\frac{e^{-\omega\tau}}{\hbar\beta}|_{\omega=i\omega_n}$ is the momentum-integrated Green's function for isolated leads per volume in the time-domain within a wide-band approximation, ν_i is the density of states per spin at Fermi level, and ω_n are fermionic Matsubara frequencies. We use this nonperturbative result only for the in-gap contributions; its evaluation in general is an open problem.

When the ABS bands, $\pm E_A(\phi)$, are well gapped from the continuum [24,25], and the charging energy is small ($E_C = e^2/2C_\Sigma \ll \Delta$ leading to slow phase dynamics), the denominators of $g_i(\tau)$ can be approximated adiabatically [33] as $\sqrt{\Delta^2 - (\hbar\omega)^2} \approx \zeta = \zeta(\phi) = \sqrt{\Delta^2 - E_A(\phi)^2}$. ζ is treated as a constant within the Matsubara summation provided that the ABS bands are sufficiently flat, $E_A(\phi)\partial_\phi E_A(\phi) \ll \Delta^2 - E_A^2(\phi)$, which is the case in the weak tunneling regime $\Gamma_i \ll \Delta$. Here, $\pm E_A(\phi)$ are the in-gap ABS levels [34] obtained from the poles of $G_{dd}(\omega)$ in the static limit, $\partial_\tau\phi_i(\tau) \to 0$. Within this approximation and at low temperatures, $\hbar\beta \gg 1/|\omega|$, $G_{dd}^{-1}(\tau,\tau') \approx G_{dd,\mathrm{a}}^{-1}(\tau)\delta(\tau - \tau')$ becomes local in time,

$$G_{dd,\mathrm{a}}^{-1}(\tau) = -\frac{1}{Z_d}\left(\hbar\partial_\tau + Z_d\left[\sum_{i=L,R} -\frac{\Gamma_i}{\zeta}\frac{i\hbar\partial_\tau\phi_i(\tau)}{2}\tau_z\right.\right.$$
$$\left.\left.+\frac{\Gamma_i\Delta}{\zeta}e^{i\tau_z\frac{\phi_i(\tau)}{2}}\tau_x e^{-i\tau_z\frac{\phi_i(\tau)}{2}} + \epsilon_g\tau_z\right]\right), \quad (6)$$

where $\Gamma_i \equiv \pi\nu_i t_i^2$ and $\frac{1}{Z_d} \equiv 1 + \frac{\Gamma}{\zeta}$ [35]. Upon substituting this result into Eq. (5), the first term in the action S_E produces a Hamiltonian that is in agreement with Ref. [18], in which phases were treated as classical parameters and the $\propto \dot{\phi}(t)$ term was obtained as a diabatic correction.

V. CONTRIBUTIONS OF THE FILLED CONTINUUM

We calculate the contribution from the negative continuum energies at zero-temperature perturbatively in t_i, in the regime $\Gamma_i \ll \sqrt{\Delta^2 - \epsilon_g^2}$. At energies $|\hbar\omega| \geqslant \Delta$, the $D(\tau)$ field is a fast variable and can be integrated out, along with the fields of the leads $\psi_i(\boldsymbol{k},\tau)$ [21,22], to obtain the leading order contribution from the continuum

$$S_T^{(2)} = \frac{1}{2}\mathrm{Tr}\int_0^{\hbar\beta}\int_0^{\hbar\beta}d\tau d\tau' G_0(\tau - \tau')\delta G^{-1}(\tau')$$
$$\times G_0(\tau' - \tau)\delta G^{-1}(\tau) \quad (7)$$

(in time domain). Here, $\delta G^{-1}(\tau)$ is the off-diagonal tunneling part of $G^{-1}(\tau)$ in Eq. (4), and $G_0(\tau) = \mathrm{diag}(\mathcal{V}_L g_L(\tau), \mathcal{V}_R g_R(\tau), g_d(\tau))$ contains the momentum-integrated Green's functions of the uncoupled leads and dot.

In order to evaluate $G_0(\tau)$, we first evaluate $g_i(\tau)$. At low temperatures, $\hbar\beta \gg \hbar/\Delta$, $g_i(\tau) \approx -\nu_i\Delta\frac{1}{\hbar}[\mathrm{sgn}(\tau)K_1(|\tau|\frac{\Delta}{\hbar}) + K_0(|\tau|\frac{\Delta}{\hbar})\tau_x]$ where $K_{0,1}(x)$ are the modified Bessel functions of the second kind. Similarly, $g_d(\tau) = -\frac{1}{\hbar}\mathrm{sgn}(\tau)e^{-\frac{\epsilon_g\tau_z}{\hbar}\tau}$. Because $K_{0,1}(|\tau|\frac{\Delta}{\hbar})$ decay exponentially for $|\tau| \gg \hbar/\Delta$, we expand the rest of the integrand in the expression for $S_T^{(2)}$ in powers of $\delta\tau = \tau - \tau'$ around $\bar{\tau} = \frac{\tau+\tau'}{2}$ [22,36]. After expanding the phases $\phi_i(\tau) - \phi_i(\tau') = \partial_{\bar{\tau}}\phi(\bar{\tau})\delta\tau + \mathcal{O}(\delta\tau^3)$ and the exponent containing phases up to second order in $\delta\tau$, we integrate out $\delta\tau$. The negative continuum contributions to each ABS are extracted as $S^{(2)}_{\rm cont} = \frac{1}{2}(S^{(2)}_T[\phi_L, \phi_R, \epsilon_g] - S^{(2)}_T[0,0,0])$,

$$S^{(2)}_{\rm cont} \approx \sum_i \int_0^{\hbar\beta} d\bar\tau \left(U^c_i - q^c_i \frac{\hbar}{e} i\partial_{\bar\tau}\phi_i(\bar\tau) + \frac{C^c_i}{2}\left[\frac{\hbar}{2e}\partial_{\bar\tau}\phi_i(\bar\tau)\right]^2\right),$$

$$U^c_i = -\Gamma_i \frac{2}{\pi}\epsilon_g \frac{\arcsin\frac{\epsilon_g}{\Delta}}{\sqrt{\Delta^2-\epsilon_g^2}}, \qquad q^c_i = -\Gamma_i e \frac{\epsilon_g + \Delta^2 \frac{\arcsin\frac{\epsilon_g}{\Delta}}{\sqrt{\Delta^2-\epsilon_g^2}}}{\pi(\Delta^2-\epsilon_g^2)}, \qquad C^c_i = \Gamma_i 2e^2 \frac{2\Delta^2+\epsilon_g^2+3\Delta^2\epsilon_g\frac{\arcsin\frac{\epsilon_g}{\Delta}}{\sqrt{\Delta^2-\epsilon_g^2}}}{\pi(\Delta^2-\epsilon_g^2)^2} \tag{8}$$

within the slow phase approximation $|i\hbar\partial_{\bar\tau}\phi_i(\bar\tau)| \ll \Delta - |\epsilon_g|$ for $|\epsilon_g| < \Delta$, and U^c_i, q^c_i, C^c_i respectively determine the energy shift, charge offset, and capacitance renormalizations for each lead. The dynamic contributions, $\propto q^c_i, C^c_i$, are associated with effects of quantum phase fluctuations, see Eq. (11) below. In a circuit representation, C^c_i is a capacitance that is in parallel to capacitances between the dot and the leads (like C_{bi} in Fig. 1).

Higher order corrections in the slow phase approximation become significant as $|\epsilon_g|$ approaches Δ; for typical gatemon values $E_C/h \lesssim 0.5$ GHz and $\Delta/h \sim 40$–50 GHz, [24,25], the above expression remains adequate for $|\epsilon_g| \lesssim 0.7\Delta$ (with a truncation error up to $\approx$5%).

$S^{(2)}_T$ corresponds to a sum of bubble diagrams that can be interpreted as the creation (at time τ) and annihilation (at time τ') of virtual particle-hole pairs by two tunneling events, with one of the pair located at either of the leads experiencing a potential $\pm eV_i(\tau)$ and the other at the dot experiencing $\mp\epsilon_g$ for a duration $|\tau'-\tau| \lesssim \frac{\hbar}{\Delta-|\epsilon_g|}$. This results in the $V_i(\tau)$-dependent (quadratic, due to expansion in $\delta\tau$) and ϵ_g-dependent contributions to the ABS energies obtained above.

We have so far obtained the leading order correction to the capacitance and charge offset. The lack of $\phi_i(\tau)$ dependence in $S^{(2)}_{\rm cont}$ is expected, since it is of second order in tunneling. In order to capture the leading order corrections to the supercurrent, we calculate the next order term in the tunnelings by neglecting phase fluctuations, $\frac{S^{(4)}_T}{\hbar} = \sum_n \frac{1}{4}{\rm Tr}([G_0(i\omega_n)\delta G^{-1}]^4)$. This static treatment disregards next order contributions to the capacitance and charge offset that come with an additional smallness factor $\sim\Gamma_i/\sqrt{\Delta^2-\epsilon_g^2}$. The continuum contribution is $S^{(4)}_{\rm cont} = \int_0^{\hbar\beta} d\tau\, \mathcal{U}^c(\phi(\tau))$ where

$$\mathcal{U}^c(\phi) = \frac{-2\Gamma_L\Gamma_R\Delta^2\sin^2\frac{\phi}{2} + \Gamma^2\epsilon_g^2\left(1+\frac{\Delta^2}{\Delta^2-\epsilon_g^2}\right)}{\Delta(\Delta^2-\epsilon_g^2)}. \tag{9}$$

For larger $\epsilon_g \lesssim \Delta$, the contribution of this term to the supercurrent can become as important as the in-gap contributions $[\partial_\phi E_A(\phi) \sim \partial_\phi \mathcal{U}^c(\phi)]$.

The combined energy shift defined as the static portions of $S^{(2)}_{\rm cont}$ and $S^{(4)}_{\rm cont}$ is given by $E_{\rm cont}(\phi) \equiv \sum_{i=L,R} U^c_i + \mathcal{U}^c(\phi)$, which is in numerical agreement with the nonperturbative result given in Eq. (12) of Ref. [18] for $\Gamma_i \ll \sqrt{\Delta^2-\epsilon_g^2}$. For $\Gamma_i, \epsilon_g \ll \Delta$, it simplifies to

$$E_{\rm cont}(\phi) \approx -\frac{2}{\pi}\Gamma\frac{\epsilon_g^2}{\Delta^2} - \frac{2\Gamma_L\Gamma_R}{\Delta}\left(1+\frac{\epsilon_g^2}{\Delta^2}\right)\sin^2\frac{\phi}{2} + \frac{2\Gamma^2\epsilon_g^2}{\Delta^3}. \tag{10}$$

VI. PHASE QUANTIZATION: CONVERTING PATH INTEGRAL TO QUANTUM HAMILTONIAN

Combining the in-gap and continuum contributions results in the effective action: $S_{\rm ABS} = \int_0^{\hbar\beta} d\bar\tau \bar D(\bar\tau)[-G^{-1}_{dd,{\rm a}}(\bar\tau)]D(\bar\tau) + S^{(2)}_{\rm cont} + S^{(4)}_{\rm cont} - \frac{C_\Sigma}{2}(\frac{\hbar}{2e}i\partial_\tau\phi(\tau) + \frac{C_I}{2C_\Sigma}V^a)^2$. At this point, it is convenient to express the action in terms of difference and average phases $\phi(\bar\tau)$ and $\phi_{\rm av}(\bar\tau) = \frac{\phi_L(\bar\tau)+\phi_R(\bar\tau)}{2}$. The weakly coupled $\phi(\tau)$ and $\phi_{\rm av}(\tau)$ fields can be decoupled perturbatively, and the confinement potential of $\phi_{\rm av}(\tau)$ can be gauged away. It can be shown that the partition function obtained from the Hamiltonian

$$\hat H = 4\tilde E_C(\hat n - \tilde n_g - n_z\hat D^\dagger\tau_z\hat D)^2 + E_{\rm cont}(\phi) + Z_d\hat D^\dagger\left(\frac{\Delta}{\zeta}\left[\Gamma\cos\frac{\hat\phi}{2}\tau_x - \delta\Gamma\sin\frac{\hat\phi}{2}\tau_y\right] + \epsilon_g\tau_z\right)\hat D, \tag{11}$$

is $Z_G \propto \int \mathcal{D}\phi e^{-S_{\rm ABS}/\hbar}$. The average phase $\hat\phi_{\rm av}(\tau)$ does not appear in $\hat H$, since its conjugate charge operator commutes with $\hat H$, which allows $\hat\phi_{\rm av}(\tau)$ to be replaced with a constant. Above, $\hat n$ and $\hat\phi$ are conjugate quantum operators satisfying $[\hat\phi, \hat n] = i$ as a result of the mapping of the functional integration over $\phi(\tau)$ onto operator formalism, and $\hat D = (\hat d_\uparrow, \hat d^\dagger_\downarrow)^T$ is the dot field operator in Nambu space. The charging Hamiltonian contains the charging energy $\tilde E_C = \frac{e^2}{2(C_\Sigma+\delta C_\Sigma)}$ with

$$\delta C_\Sigma(\epsilon_g) = \left[(C^c_L)^{-1} + (C^c_R)^{-1}\right]^{-1}, \tag{12a}$$

$$n_z(\epsilon_g) = \frac{C_\Sigma + \frac{C^c_L+C^c_R}{4}}{C_\Sigma+\delta C_\Sigma}\frac{\delta\Gamma}{4(\zeta+\Gamma)}, \tag{12b}$$

$$\tilde n_g(\epsilon_g) = \frac{C_\Sigma + \frac{C^c_L+C^c_R}{4}}{C_\Sigma+\delta C_\Sigma}\left(n_g + \frac{q^c_L - q^c_R}{2e}\right), \tag{12c}$$

where $n_g = \frac{1}{2e}\frac{C_I}{2}V^a$ is the usual charge offset owing to an applied voltage (see Fig. 1), $n_z(\epsilon_g)$ is the strength of the charge offset term that depends on the dot occupation, and $\delta n_g(\epsilon_g) \simeq \tilde n_g(\epsilon_g) - n_g \approx \frac{q^c_L-q^c_R}{2e}$ is the charge offset induced by the continuum contributions from Eq. (8), and $\delta\Gamma = \Gamma_L - \Gamma_R$.

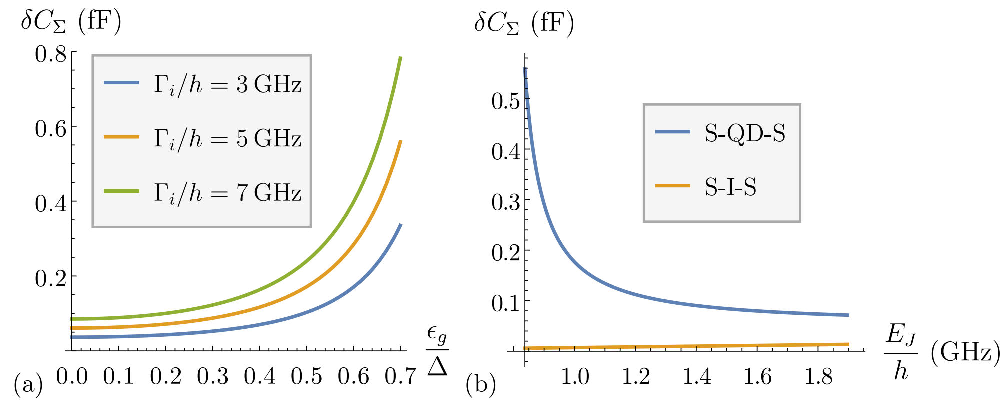

FIG. 2. (a) Change in effective shunting capacitance across the junction δC_Σ as a function of gate voltage ϵ_g for a set of representative values of Γ_i at $\Delta/h = 45$ GHz. (b) A comparison of δC_Σ for S-QD-S junction, Eq. (12a), at low transparencies T, and the analogous value of $\delta C_\Sigma^{\rm JJ} = \frac{3e^2}{8\Delta^2}E_J$ for an S-I-S junction [22] at given values E_J. For the S-QD-S curve, an effective E_J is defined via Eq. (17) as ϵ_g/Δ is varied between 0.2 and 0.7 for $\Gamma_i/h = 5$ GHz. In a typical S-I-S junction used for transmon with many channels, the value of E_J/h is ~10 GHz [37].

In Fig. 2(a), the change in capacitance δC_Σ is shown as a function of $\epsilon_g \in [0, 0.7\Delta]$ for a few representative values $\Gamma_i \ll \sqrt{\Delta^2 - \epsilon_g^2}$. As an example of the charge offsets [38] $n_z(\epsilon_g)$ and $\delta n_g(\epsilon_g)$ given by Eqs. (12b) and (12c), which arise in asymmetric junctions, their values for $\epsilon_g = 0.7\Delta$, $\Gamma_L/h = 5$ GHz and $\Gamma_R/h = 1$ GHz are, respectively, 0.02 and −0.05.

Since the parity operator $(\hat{D}^\dagger \tau_z \hat{D})^2$ commutes with $\hat{H}$, the even- and odd-parity sectors are decoupled [39]. Projecting Eq. (11) onto the even occupancy states $|0\rangle$ and $|\uparrow\downarrow\rangle = d_\uparrow^\dagger d_\downarrow^\dagger |0\rangle$, we obtain

$$\hat{H}_{\rm even} = 4\tilde{E}_C(-i\partial_\phi - \tilde{n}_g - n_z\eta_z)^2 + \hat{U}_J(\phi), \tag{13}$$

where $\hat{U}_J$ is the 2×2 Josephson matrix potential, which includes in-gap (ABS) and continuum contributions,

$$\hat{U}_J(\phi) = Z_d\left(\frac{\Delta}{\zeta}\left[\Gamma\cos\frac{\phi}{2}\eta_x - \delta\Gamma\sin\frac{\phi}{2}\eta_y\right] + \epsilon_g\eta_z\right) + E_{\rm cont}(\phi), \tag{14}$$

where $Z_d \equiv \frac{\zeta}{\zeta+\Gamma}$, and $\eta_{x,y,z}$ are the Pauli matrices acting on the even occupancy space of the dot. To the second order in t_i, qualitatively, for a doubly occupied (unoccupied) dot either (i) a single electron (hole) can tunnel to a lead and back or (ii) a pair of electrons (holes) can cotunnel to one of the leads. Since electrons and holes differ in charge, the first process will generally lead to occupancy dependent charge offset, since $\propto n_z\eta_z$. The second process corresponds to change of the dot occupancy, reflected in the off-diagonal terms of Eq. (13). When one of the leads is disconnected from the dot, the phase dependence of $\hat{H}_{\rm even}$ can be removed and the supercurrent vanishes.

To compare to a typical S-I-S JJ we consider a low-transparency regime in Eq. (13) where the charging energy will be neglected. The eigenvalues of the potential term $\propto Z_d$ in $\hat{H}_{\rm even}$ yields the well-known result for the in-gap ABS energies [34]

$$E_A(\phi) = \frac{\Delta}{\zeta+\Gamma}\sqrt{\Gamma^2 + \frac{\epsilon_g^2\zeta^2}{\Delta^2}}\sqrt{1 - T(\epsilon_g)\sin^2\frac{\phi}{2}}, \tag{15}$$

where we defined the transparency as

$$T(\epsilon_g) \equiv \frac{4\Gamma_L\Gamma_R}{\Gamma^2 + \epsilon_g^2\frac{\zeta^2}{\Delta^2}}. \tag{16}$$

In the regime of small $\Gamma_i \ll \sqrt{\Delta^2 - \epsilon_g^2}$ and small ϵ_g, $T(\epsilon_g)$ takes the Breit–Wigner form (cf. Ref. [24]). In the low-transparency limit, $T \ll 1$, (reached either for $\Gamma_L \gg \Gamma_R$ or for relatively large gate voltages, ϵ_g), ABS are well gapped allowing to obtain an effective Josephson energy

$$E_{J,\rm eff}^A \approx \frac{\Delta}{\zeta+\Gamma}\frac{\Gamma_L\Gamma_R}{\sqrt{\Gamma^2 + \frac{\epsilon_g^2\zeta^2}{\Delta^2}}}. \tag{17}$$

In Fig. 2(b), we use this definition to make a comparison between δC_Σ for an S-QD-S junction, and the analogous $\delta C_\Sigma^{\rm JJ}$ for an S-I-S junction at a given value of E_J [22], which shows that the capacitance renormalization is one to two orders of magnitude stronger for the S-QD-S junction [40].

VII. DISCUSSION AND OUTLOOK

In this paper we have developed a self-consistent approach, reducing the underlying many-body system of a S-QD-S junction to a simple Hamiltonian of a single variable—the phase difference across the junction. When the S-QD-S junction is shunted by capacitance C_Σ, the phase $\hat{\phi}$ is a quantum operator and the associated charging energy E_C gets renormalized as $\tilde{E}_C = \frac{e^2}{2(C_\Sigma + \delta C_\Sigma(\epsilon_g))}$ while the Hamiltonian becomes a 2×2 matrix acting on the even occupancy states of the dot. In addition to the capacitance, the charge offset gets new QD gate voltage dependent contributions, $\delta n_g(\epsilon_g)$, $n_z(\epsilon_g)$ that arise in an asymmetric situation, when hopping rates to the left and to the right are different, $\Gamma_L \neq \Gamma_R$.

A direct experimental probe of the capacitance renormalization δC_Σ (as well as δn_g and n_z) would be to measure changes in the anharmonicity α of a gatemon while sweeping the gate voltage ϵ_g. The predicted strength of δC_Σ and its sensitive dependence on ϵ_g suggests that it could be important to account for when designing high-fidelity quantum gates, e.g., in architectures utilizing ϵ_g modulation to realize entangling gates between qubits.

The new charge offsets $\tilde{n}_g$ and n_z that arise for asymmetric tunnelings $\Gamma_L \neq \Gamma_R$, and their dependence on ϵ_g and Γ_i will be important in the interpretation of previous [24–26] and new experiments, e.g., Refs. [14,15], in this growing field of quantum circuits based on super-semi junctions. The ϵ_g and Γ_i dependence of the new offset charges n_z and δn_g could also be the basis for coupling super-semi junction circuits to each other or to a general circuit environment in new ways.

From a theoretical standpoint, it is desirable to extend our method to the strong tunneling regime, $\Gamma_i \sim \Delta$, e.g., in a nonperturbative approach, to obtain higher-order corrections to time-dependent continuum contributions, like $S^{(4)}_{\rm cont}$ (that would lead to phase-dependent corrections to the capacitance). Also note that nonperturbative calculations for n_z [38] and $E_{\rm cont}(\phi)$ [18,41] show they can grow by an order of magnitude in the strong tunneling regime. These results are also relevant to treat multiterminal devices [14], and to explicitly include multichannel physics that is particularly relevant for planar super-semi junctions [42–44].

ACKNOWLEDGMENTS

We acknowledge helpful discussions with Pavel D. Kurilovich, Max Hays, Thomas Hazard, and Emily Toomey. This research was funded by the LPS Qubit Collaboratory, and in part under Air Force Contract No. FA8702-15-D-0001. Any opinions, findings, conclusions or recommendations expressed in this material are those of the authors and do not necessarily reflect the views of the U.S. Air Force or the U.S. Government.

[1] M. Kjaergaard, M. E. Schwartz, J. Braumüller, P. Krantz, J. I.-J. Wang, S. Gustavsson, and W. D. Oliver, Superconducting qubits: Current state of play, Annu. Rev. Condens. Matter Phys. **11**, 369 (2020).

[2] S. Bravyi, O. Dial, J. M. Gambetta, D. Gil, and Z. Nazario, The future of quantum computing with superconducting qubits, J. Appl. Phys. **132**, 160902 (2022).

[3] J. Koch, T. M. Yu, J. Gambetta, A. A. Houck, D. I. Schuster, J. Majer, A. Blais, M. H. Devoret, S. M. Girvin, and R. J. Schoelkopf, Charge-insensitive qubit design derived from the Cooper pair box, Phys. Rev. A **76**, 042319 (2007).

[4] J. E. Mooij, T. P. Orlando, L. Levitov, L. Tian, C. H. van der Wal, and S. Lloyd, Josephson persistent-current qubit, Science **285**, 1036 (1999).

[5] V. E. Manucharyan, J. Koch, L. I. Glazman, and M. H. Devoret, Fluxonium: Single cooper-pair circuit free of charge offsets, Science **326**, 113 (2009).

[6] A. Gyenis, P. S. Mundada, A. Di Paolo, T. M. Hazard, X. You, D. I. Schuster, J. Koch, A. Blais, and A. A. Houck, Experimental realization of a protected superconducting circuit derived from the $0-\pi$ qubit, PRX Quantum **2**, 010339 (2021).

[7] T. W. Larsen, K. D. Petersson, F. Kuemmeth, T. S. Jespersen, P. Krogstrup, J. Nygård, and C. M. Marcus, Semiconductor-nanowire-based superconducting qubit, Phys. Rev. Lett. **115**, 127001 (2015).

[8] G. de Lange, B. van Heck, A. Bruno, D. J. van Woerkom, A. Geresdi, S. R. Plissard, E. P. A. M. Bakkers, A. R. Akhmerov, and L. DiCarlo, Realization of microwave quantum circuits using hybrid superconducting-semiconducting nanowire Josephson elements, Phys. Rev. Lett. **115**, 127002 (2015).

[9] M. Pita-Vidal, A. Bargerbos, C.-K. Yang, D. J. van Woerkom, W. Pfaff, N. Haider, P. Krogstrup, L. P. Kouwenhoven, G. de Lange, and A. Kou, Gate-tunable field-compatible fluxonium, Phys. Rev. Appl. **14**, 064038 (2020).

[10] C. Janvier, L. Tosi, L. Bretheau, C. O. Girit, M. Stern, P. Bertet, P. Joyez, D. Vion, D. Esteve, M. F. Goffman, H. Pothier, and C. Urbina, Coherent manipulation of Andreev states in superconducting atomic contacts, Science **349**, 1199 (2015).

[11] M. Hays, G. de Lange, K. Serniak, D. J. van Woerkom, D. Bouman, P. Krogstrup, J. Nygård, A. Geresdi, and M. H. Devoret, Direct microwave measurement of Andreev-bound-state dynamics in a semiconductor-nanowire Josephson junction, Phys. Rev. Lett. **121**, 047001 (2018).

[12] M. Hays, V. Fatemi, D. Bouman, J. Cerrillo, S. Diamond, K. Serniak, T. Connolly, P. Krogstrup, J. Nygård, A. L. Yeyati, A. Geresdi, and M. H. Devoret, Coherent manipulation of an Andreev spin qubit, Science **373**, 430 (2021).

[13] M. Pita-Vidal, A. Bargerbos, R. Žitko, L. J. Splitthoff, L. Grünhaupt, J. J. Wesdorp, Y. Liu, L. P. Kouwenhoven, R. Aguado, B. van Heck, A. Kou, and C. K. Andersen, Direct manipulation of a superconducting spin qubit strongly coupled to a transmon qubit, Nat. Phys. **19**, 1110 (2023).

[14] F. J. Matute-Cañadas, L. Tosi, and A. L. Yeyati, Quantum circuits with multiterminal Josephson-Andreev junctions, PRX Quantum **5**, 020340 (2024).

[15] D. M. Pino, R. S. Souto, and R. Aguado, Minimal Kitaev–transmon qubit based on double quantum dots, Phys. Rev. B **109**, 075101 (2024).

[16] C. W. J. Beenakker and H. van Houten, Josephson current through a superconducting quantum point contact shorter than the coherence length, Phys. Rev. Lett. **66**, 3056 (1991).

[17] A. Zazunov, V. S. Shumeiko, E. N. Bratus', J. Lantz, and G. Wendin, Andreev level qubit, Phys. Rev. Lett. **90**, 087003 (2003).

[18] P. D. Kurilovich, V. D. Kurilovich, V. Fatemi, M. H. Devoret, and L. I. Glazman, Microwave response of an Andreev bound state, Phys. Rev. B **104**, 174517 (2021).

[19] K. K. Likharev, *Dynamics of Josephson Junctions and Circuits* (CRC Press, Boca Raton, FL, 1986).

[20] M. H. Devoret, Quantum fluctuations in electrical circuits, in *Quantum Fluctuations: Les Houches Session LXIII, June 27 to July 28 1995*, edited by E. G. S. Reynaud and J. Zinn-Justin (Elsevier, Amsterdam, 1997), pp. 351–386.

[21] V. Ambegaokar, U. Eckern, and G. Schön, Quantum dynamics of tunneling between superconductors, Phys. Rev. Lett. **48**, 1745 (1982).

[22] U. Eckern, G. Schön, and V. Ambegaokar, Quantum dynamics of a superconducting tunnel junction, Phys. Rev. B **30**, 6419 (1984).

[23] A. I. Larkin and Y. N. Ovchinnikov, Decay of the supercurrent in tunnel junctions, Phys. Rev. B **28**, 6281 (1983).

[24] A. Kringhøj, B. van Heck, T. W. Larsen, O. Erlandsson, D. Sabonis, P. Krogstrup, L. Casparis, K. D. Petersson, and C. M. Marcus, Suppressed charge dispersion via resonant tunneling in a single-channel transmon, Phys. Rev. Lett. **124**, 246803 (2020).

[25] A. Bargerbos, W. Uilhoorn, C.-K. Yang, P. Krogstrup, L. P. Kouwenhoven, G. de Lange, B. van Heck, and A. Kou, Observation of vanishing charge dispersion of a nearly open superconducting Island, Phys. Rev. Lett. **124**, 246802 (2020).

[26] T. Vakhtel and B. van Heck, Quantum phase slips in a resonant Josephson junction, Phys. Rev. B **107**, 195405 (2023).

[27] Assuming the dot's energy quantization provides the largest energy scale, $\delta E \gg \Delta, U$, scf. [18].

[28] P. Coleman, *Introduction to Many-Body Physics* (Cambridge University Press, Cambridge, 2015).

[29] A. Altland and B. Simons, *Condensed Matter Field Theory, Second Edition*, 2nd ed. (Cambridge University Press, Cambridge, 2010).

[30] A. V. Rozhkov and D. P. Arovas, Josephson coupling through a magnetic impurity, Phys. Rev. Lett. **82**, 2788 (1999).

[31] V. Meden, The Anderson-Josephson quantum dot-a theory perspective, J. Phys.: Condens. Matter **31**, 163001 (2019).

[32] D. O. Oriekhov, Y. Cheipesh, and C. W. J. Beenakker, Voltage staircase in a current-biased quantum-dot Josephson junction, Phys. Rev. B **103**, 094518 (2021).

[33] A. Zazunov, V. S. Shumeiko, G. Wendin, and E. N. Bratus', Dynamics and phonon-induced decoherence of Andreev level qubit, Phys. Rev. B **71**, 214505 (2005).

[34] C. Beenakker and H. van Houten, The superconducting quantum point contact, *Nanostructures and Mesoscopic Systems* (Elsevier, Amsterdam, 1992), pp. 481–497.

[35] For $\Gamma_i \ll \sqrt{\Delta^2 - \epsilon_g^2}$, $\zeta(\phi)$ depends weakly on the phase, $\zeta = \sqrt{\Delta^2 - \epsilon_g^2} + \Gamma \frac{\epsilon_g^2}{\Delta^2 - \epsilon_g^2} + \mathcal{O}(\frac{\Gamma_i^2}{\Delta^2 - \epsilon_g^2} \sin^2 \frac{\phi}{2})$.

[36] U. Eckern, M. Gruber, and P. Schwab, Effective descriptions of complex quantum systems: Path integrals and operator ordering problems, Ann. Phys. (Leipzig) **517**, 578 (2005).

[37] C. Berke, E. Varvelis, S. Trebst, A. Altland, and D. P. DiVincenzo, Transmon platform for quantum computing challenged by chaotic fluctuations, Nat. Commun. **13**, 2495 (2022).

[38] The occupation-dependent charge offset $(2e)n_z$ is nonperturbative in $\Gamma_{L,R}$. n_z originates from the $\partial_\tau \phi(\tau)$-term in Eq. (6); it can reach $e/2$ for $\Gamma_{L,R} \gg \Delta$ and $\delta\Gamma \sim \Gamma$.

[39] By projecting onto the odd parity subspace, $\{|\uparrow\rangle, |\downarrow\rangle\}$, we obtain $\hat{H}_{\rm odd} = 4\tilde{E}_C(-i\partial_\phi - \tilde{n}_g)^2 + E_{\rm cont}(\phi)$, which is relevant when the Coulomb interaction is negligible.

[40] A more rigorous definition of $E_{J,\rm eff}$ with exact continuum contributions does not alter this result.

[41] V. Fatemi, P. D. Kurilovich, A. R. Akhmerov, and B. van Heck, Nonlinearity of transparent SNS weak links decreases sharply with length, SciPost Phys. **18**, 091 (2025).

[42] L. Casparis, M. R. Connolly, M. Kjaergaard, N. J. Pearson, A. Kringhøj, T. W. Larsen, F. Kuemmeth, T. Wang, C. Thomas, S. Gronin *et al.*, Superconducting gatemon qubit based on a proximitized two-dimensional electron gas, Nat. Nanotechnol. **13**, 915 (2018).

[43] W. M. Strickland, L. J. Baker, J. Lee, K. Dindial, B. H. Elfeky, P. J. Strohbeen, M. Hatefipour, P. Yu, I. Levy, J. Issokson, V. E. Manucharyan, and J. Shabani, Characterizing losses in InAs two-dimensional electron gas-based gatemon qubits, Phys. Rev. Res. **6**, 023094 (2024).

[44] S. Liu, A. Bordoloi, J. Issokson, I. Levy, M. G. Vavilov, J. Shabani, and V. Manucharyan, Strongly-anharmonic gateless gatemon qubits based on InAs/Al 2D heterostructure, arXiv:2503.12288.